Catalog Build-Up for Geostationary Orbit Using Simulated Short-Arc Tracklets

Jan A. Siminski, Martin Weigel, Hauke Fiedler
German Aerospace Center (DLR), German Space Operations Center,
Space Situational Awareness Group, Münchner Str. 20, 82234 Weßling, Germany.

ABSTRACT

In order to guarantee save operation of satellites in the geostationary orbit, space object databases are created. Close encounters between uncontrollable and active objects must be detected and maneuvers must be planned to avoid future collisions.
The geostationary orbit is typically monitored using ground-based optical telescopes. They are operated in a surveillance mode, i.e. the entire region is covered by the observation strategy to ensure a complete catalog. Due to limited resources, objects can only be observed for short durations. The resulting measurement arcs, called tracklets, do not provide enough information to determine the full state of the objects.
When building up the database using no prior information, tracklets must be associated to each other to obtain object candidates. An efficient method was developed for this task, which optimally uses the information contained in the short sequences of angular measurements, i.e. the line-of-sights and their derivative. The resulting candidate solutions are either confirmed and refined with further observations or rejected.

This work will examine whether it is feasible to build up a catalog using the developed algorithms and short tracklets as observations. A simulation of an optical sensor network is performed. Near-geostationary objects are extracted from publicly available catalogs. The developed method is then used to generate the catalog. The resulting object database is analyzed for accuracy and completeness. The study will outline the performance of such a system and identify deficiencies.

1. INTRODUCTION

The German Space Operations Center (GSOC) builds up a small aperture robotic telescope system in Sutherland, South Africa. It will be assembled and operated in collaboration with the Astronomical Institute of the University of Bern.
The system will consist of two telescopes on one mount, where each telescope is used for a different operational mode: surveillance or tracking. Details on the setup can be obtained from [1].
When combining the data from the telescope in South Africa with measurements taken from the Zimmerwald observatory in Switzerland, the near-geostationary orbit domain for European longitudes can be covered on a regular basis and independent on the season.

In order to build up a catalog, the surveillance mode is used which scans the complete orbital domain for new objects. The new surveillance telescope has a field of view of about 2°. Due to the limited field of view and the large orbital region, each object can only be observed for short durations, even when using the two observatories.
These short observation arcs are commonly known as tracklets. If a new object is detected, the measurements must be associated to other tracklets to obtain new object candidates. This task is particularly important during the first build-up of the catalog but also later when objects are lost, e.g. after they have been maneuvered.

In previous work an approach for this task is presented which uses a boundary-value formulation of the tracklet association problem [2]. The method is briefly explained in section 2. The previous research studied the association performance of the method, i.e. how well does it link observations of common objects while keeping the false-association rate small. This work focuses on the accuracy of the generated object candidates. The object candidates can only be associated to further measurements if the orbital solution is close to the actual one. When using traditional orbit improvement methods, e.g. batch or sequential estimation, the convergence largely dependents on the accuracy of the initial estimate. Thus, an accuracy study is performed in section 3, where realistic measurements are generated using the prospective telescope setup in Zimmerwald and Sutherland. The last section will discuss the results and give a conclusion.

1.1 Tracklet association problem

Tracklets contain a series of angular pairs, namely right ascension α and declination δ values. The information of the measurement arc is reduced to the line-of-sight $\mathbf{u}$ and its derivative $\dot{\mathbf{u}}$ by fitting a motion model to the angles. It is commonly expressed using angles and angular rates at a mean epoch

$$\mathbf{a} = (\alpha, \delta, \dot{\alpha}, \dot{\delta})^{\mathsf{T}} , \tag{1}$$

where the variable $\mathbf{a}$ is named attributable vector. The orbit of an object is fully described by six independent parameters, e.g. orbital elements or a state vector

$$\mathbf{y}(t) = (\mathbf{r}(t), \dot{\mathbf{r}}(t))^{\mathsf{T}} . \tag{2}$$

The attributable lacks complete orbital information as it only constraints four degrees of freedom. Thus, two tracklets are required to perform an initial orbit determination.
An orbit can be determined given boundary values, e.g. the geocentric positions at two observation epochs

$$\mathbf{r}(t_1) = \mathbf{r}_1 \text{ and } \mathbf{r}(t_2) = \mathbf{r}_2 . \tag{3}$$

The corresponding orbit $\mathbf{y}(t)$ is computed using Lambert's problem solvers, e.g. by Battin [3] or Gooding [4]. However, multiple solutions exist depending on the path taken in between the measurements epochs. In order to uniquely define one orbital solution an additional parameter k is required, i.e. the number of completed half and full revolutions. Hence, the orbit is completely defined by

$$\mathbf{y}(t, \mathbf{r}_1, \mathbf{r}_2, k). \tag{4}$$

Traditional Lambert's problem solvers account only for two-body dynamics. Computationally more expensive approaches use so called shooting methods and high-fidelity force models to compute the connecting orbit.
The required geocentric positions can be described in terms of the observed variables

$$\mathbf{r} = \mathbf{r}_S + \rho \cdot \mathbf{u}(\alpha, \delta) . \tag{5}$$

Here, ρ denotes the topocentric range and $\mathbf{r}_S$ the location of the optical sensor. Thus, given two line-of-sights $\mathbf{u}_1$ and $\mathbf{u}_2$ and the respective ranges ρ_1 and ρ_2 an orbit for each feasible k can be computed

$$\mathbf{y}(t, \rho_1, \rho_2, k, \mathbf{z}) , \tag{6}$$

where

$$\mathbf{z} = (\alpha_1, \delta_1, \alpha_2, \delta_2)^{\mathsf{T}} . \tag{7}$$

Fig. 1 illustrates the general tracklet association and initial orbit determination problem. An orbit hypothesis defined by two range values connects the two measurement arcs.

2. METHODOLOGY

Various methods have been published which use this boundary-value formulation of the tracklet association problem, e.g. see [5,6,7]. They typically compute orbits for two range hypotheses and test these solutions against further measurements. In [5] hypotheses are selected on a regular grid, i.e. all possible (ρ_1, ρ_2) - hypotheses in an admissible region. References [6,7] sample the hypothesis space using statistical approaches. If the orbits are verified they create catalog objects, otherwise the hypotheses are rejected.

This work uses an approach presented in [2], which makes use of the angular rates

$$\dot{\mathbf{z}} = (\dot{\alpha}_1, \dot{\delta}_1, \dot{\alpha}_2, \dot{\delta}_2)^{\mathsf{T}} \tag{8}$$

to decide which hypotheses create candidate objects. Using the dependencies in (6) and given the ranges ρ_1 and ρ_2, the modeled measurements at both observation epochs are defined by

$$\hat{\mathbf{z}}(\rho_1, \rho_2, k, \mathbf{z}) = (\hat{\alpha}_1, \hat{\delta}_1, \hat{\alpha}_2, \hat{\delta}_2)^{\mathsf{T}}. \tag{9}$$

The modeled measurements are compared to the actual measured ones in order to test the probability of the hypothesis. The overall process is illustrated in the diagram in Fig. 2.

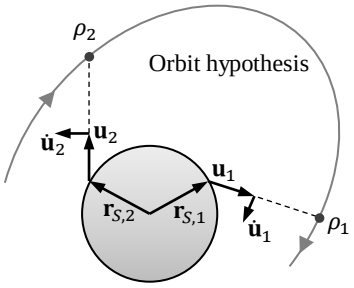

Fig. 1. Tracklet association problem [2]

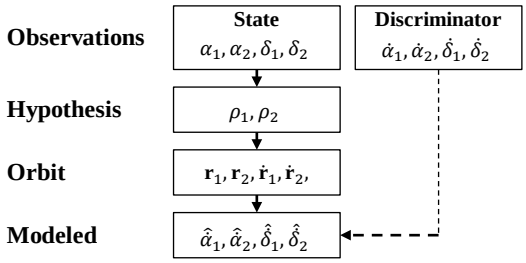

Fig. 2. Process flow of boundary-value approach [2]

Instead of testing all feasible range combinations, an optimization approach is used. A loss function is defined by

$$L(\rho_1, \rho_2, k, \mathbf{z}) = \left(\dot{\mathbf{z}} - \hat{\dot{\mathbf{z}}}\right)^{\mathsf{T}} (\mathbf{C}_{\dot{\mathbf{z}}} + \mathbf{C}_{\hat{\dot{\mathbf{z}}}}) \left(\dot{\mathbf{z}} - \hat{\dot{\mathbf{z}}}\right), \tag{10}$$

where $\mathbf{C}_{\dot{\mathbf{z}}}$ is the covariance matrix describing the uncertainty in the measured angular rates, and $\mathbf{C}_{\hat{\dot{\mathbf{z}}}}$ the uncertainty in the modeled angular rates due to the uncertainty in the measured angles.
L is minimized using gradient-based optimizers in order to find the best fitting orbital solutions to both observations. The function subtracts the modeled angular rates from the measured ones and scales the difference by its uncertainty. It has to be minimized for all feasible k values. Range hypotheses with no physically meaningful orbits can be excluded by bounding the optimization algorithm to an admissible interval. The bounds are selected similarly to [8] by defining semi-major axis and apogee-perigee limits

$$\mathcal{C}(\mathbf{z}) = \{\rho_i, i \in [1,2]: \|\mathbf{r}_{\min}\| \leq \|\mathbf{r}(\rho_i)\| \leq \|\mathbf{r}_{\max}\|,\ a_{\min} \leq a(\rho_1, \rho_2) \leq a_{\max}\}. \tag{11}$$

Each minimum is then tested against a predefined threshold to decide whether the two observations belong to a common object or not. The threshold is defined accounting that the minimization result is distributed according to the χ^2-distribution.

3. SIMULATION FRAMEWORK

The performance of the tracklet association and initial orbit determination depends on the observation geometry, e.g. the larger the orbital arc covered by the two tracklets, the more accurate information on the orbit is obtained. In order to assess the catalog build-up performance and the accuracy of candidate solutions, realistic measurements have to be generated. The magnitude of the objects is dependent on their diameter and the solar phase angle. That is why observation strategies try to optimize this angle. However, this comes with certain drawbacks, e.g. objects are likely to be re-observed at almost the same position on their orbit.

A simulation is carried out to determine realistic observations. It is explained in the following.

3.1 Simulated objects and telescopes

The simulation is performed using a set of near-geostationary satellites from the publicly available catalog[1]. The satellites were extracted using the filter settings summarized in Tab. 1. In total, 661 objects which are visible from at least one sensor are taken into account for the simulation. Two optical sensors are placed at the positions as specified in Tab. 2.

Tab. 1. Near-geostationary objects selected for simulation

Semi-major axis a	30000-50000 km
Eccentricity e	0 – 0.3
Inclination i	0 – 15°

Tab. 2. Telescope location: Longitude λ, latitude ϕ and height h.

	λ [°]	ϕ [°]	h [m]
Zimmerwald	7.465	46.877	970
Sutherland	20.813	−32.937	1700

Each telescope has a 2° field of view and a takes 20 seconds for integration and read-out. This time per frame defines the spacing between individual observations within one tracklet.

3.2 Observation plan

The telescopes run in surveillance mode, i.e. they try to cover the complete visible region of the geostationary orbit. This complete coverage is achieved by fixing a right ascension value and scanning a specified declination interval. Every object will appear on this stripe if it is observed continuously. The declination interval is narrowed accounting for the distribution of objects. Further details on the survey strategy can be obtained from [9, 10].
In order to optimize visibility conditions, right ascension values close to the Earth shadow are used. Fig. 3 illustrates two possible values. The sun direction is assumed to be constant for one night.
Instead of scanning only one stripe, four are selected, two on each side of the shadow cone. The right ascension values are determined for each night, accounting that they should not be too close to the Moon, Milky Way, and shadow cone. Additionally, the Sun elevation and phase angle are accounted when defining an observation task, i.e. stripe location for a specific observation epoch.

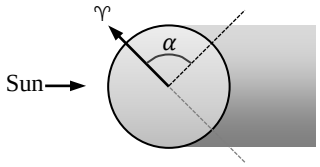

Fig. 3. Stripe selection method

The conditions for a successful observation are summarized in the following table.

Tab. 3. Conditions for successful stripe selection

Min. Moon angular distance to observed direction	20°
Min. galactic latitude of observed direction	20°
Max. Sun elevation	-12°
Max. solar phase angle	90°

This method does not give the best results in terms of re-observation times and information gain of a new tracklet. However, it can still serve as a reference strategy to test the tracklet association. An improvement in the observation strategy will then also improve the presented results.

3.3 Simulated observations

Using the previously described observation plan, the telescope pointing for each simulation step is computed. Each object that appears in the field of view at least three times in a series of five images, creates a tracklet. A tracklet consists therefore of maximal 5 individual right ascension and declination measurements. The objects are propagated to the observation epochs accounting for the simplified perturbation model (SGP4). Astrometric data reduction from the telescope images is not modelled. Instead, a random normally distributed error with $\sigma_{\alpha,\delta} = 0.7''$

[1] Space-Track.Org: “Two Line Element data set”, http://www.space-track.org, accessed 08/01/2014.

is added to each angular measurement to simulate noise. Additionally, one random error with $\sigma = 5.0''$ is added to all measurements of a tracklet representing a bias, e.g. due to false recording of the exposure epoch. These values do not represent the actual performance of the telescopes but give an approximate upper bound of the expected errors.
Failed data retrieval, due to bad weather conditions or bright stars in the image, is not yet modeled. Thus, the simulation does not provide a realistic number of observations. However, it gives a good image on the re-observation geometries, i.e. the distribution of measurements on the orbit.
Observations are generated for the whole year 2015. In total about 80.000 tracklets are collected.

4. RESULTS

The data set is processed with the tracklet association method as described in section 2. Then, the achievable accuracy of object candidates is estimated. For that purpose, the obtained orbit solutions are compared with the simulated known orbits.

All tracklets that belong to a common object are extracted from the data set. Then, each tracklet is tested against the successive one. The association is successful if the minimum of the loss function in (10), $\min L(\rho_1, \rho_2, k, \mathbf{z})$, falls below a threshold. The threshold 9.49 is used to cover the 95th percentile of the Chi-Squared distribution with 4 degrees of freedom. If an object candidate is created, the respective orbit is compared to the actual orbit by computing the difference between positions and velocities at the epoch of the first observation. Altogether, around 40.000 successful associations are found. The resulting statistics are shown in Fig. 4 and Fig. 5.

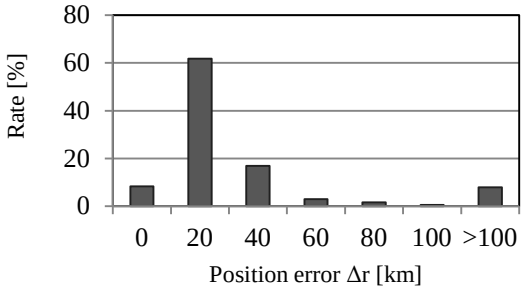

Fig. 4. Distribution of the position error

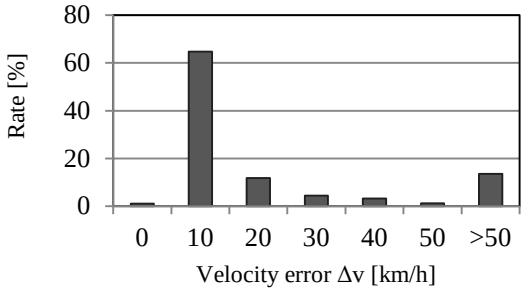

Fig. 5. Distribution of the velocity error

Due to the computational burden of shooting methods, the tested association so far only accounts for two-body dynamics. The results can be furthermore improved by including more complex Lambert's problem solvers. Still, the overall performance is quite promising, yielding a position error better than 40 km and a velocity error better than 20 km/h for around 80 percent of the tests.
However, a significant number of candidate solutions with errors larger than 100 km and 50 km/h respectively can be observed. It is difficult to link these object candidates with further measurements, thus leading to an incomplete catalog. The reason for these errors can be studied by plotting the error against the arc of the orbit covered by the two tracklets (Fig. 6 and Fig. 7).

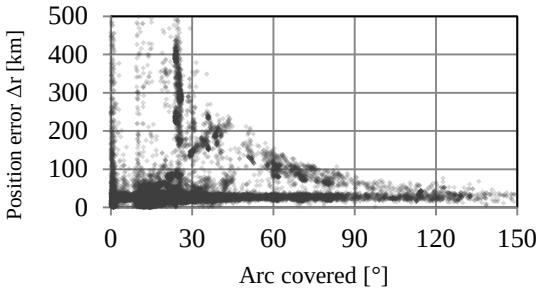

Fig. 6. Position error depending on overall arc covered by two tracklets

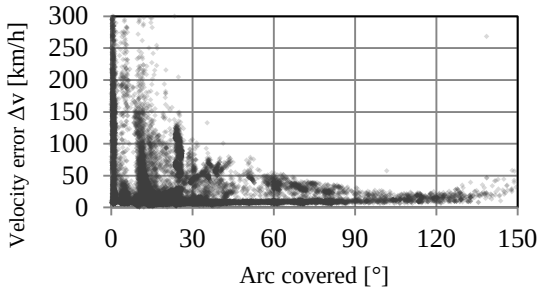

Fig. 7. Velocity error depending on overall arc covered by two tracklets

The large errors occur if a very small fraction of the orbit is covered by the tracklet combination. In order to reduce these unfavorable geometries, the observation strategy needs to be adjusted. However, the method gives enough good initial orbit estimates even using the described strategy. Additionally, the position error of the resulting objects is plotted against the orbital inclination in Fig. 8. A higher density of large errors is obtained for the highest and smallest inclination. The increase in errors for the low inclination orbits comes from the large object density in this orbital region. More objects can be observed with unfavorable geometries. The errors for objects on high inclination orbits need to be studied more in detail. They could occur due to the repeated observation of the objects at the ascending or descending node.

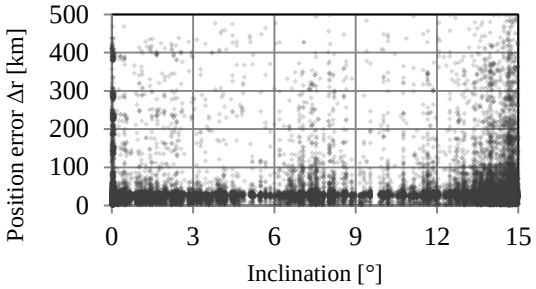

Fig. 8. Position error depending on inclination of object

To demonstrate the completeness of the theoretical catalog the number of objects with an acceptable candidate solution is compared to the number of objects without it. The candidates are assumed as good estimates if at least one solution has an error less than 100 km and 50 km/h. Fig. 9 shows the ratio of good solutions for each month of the simulated year. A seasonal variation can be observed. Around 70-80% of the observed objects can be successfully located in each month.

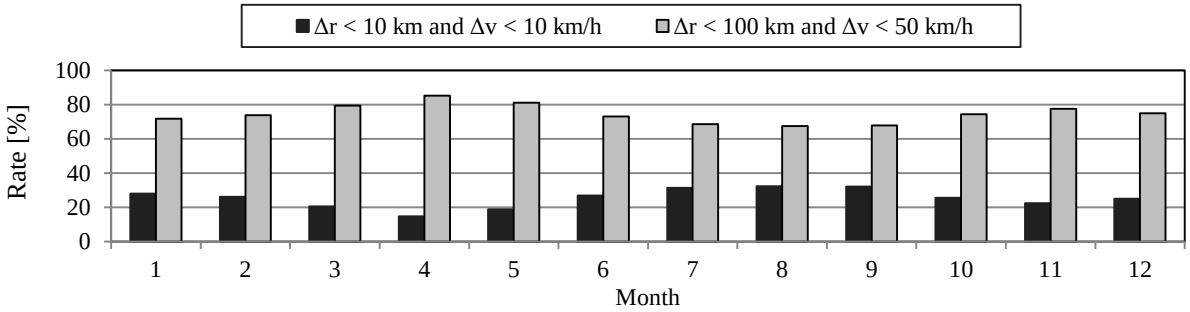

Fig. 9. Percentage of candidate objects that have been generated with an accuracy smaller than 10 km / 10 km/h or smaller than 100 km / 100 km/h

5. SUMMARY AND CONCLUSION

The catalog build-up performance, i.e. accuracy of candidate objects and the completeness of the data base, is mainly dependent on the observation strategy. Observation which capture objects on different locations of their respective orbits, lead to better candidates. The results could be pessimistic as conservative errors are assumed for the telescopes. After an analysis of the actual telescopes this model will be adjusted. However, even with the simple observation strategy used here, the overall performance of the method is convincing. The developed simulation environment can be used to improve observation schedulers. Optimal telescope schedulers have to consider the trade-off between visibility conditions and information gain, and task the observations accordingly.
Further studies will improve the tracklet error modeling, e.g. by simulating the image data reduction and accounting for further error sources. These models can then be evaluated with real observations when the telescope in South Africa is operational.

6. ACKNOWLEDGEMENTS

This work was funded by the Munich Aerospace scholarship program.

7. REFERENCES

1. Herzog, J., Fiedler, H., Weigel, M., Montenbruck, O., Schildknecht, T., SMARTnet: A sensor for monitoring the geostationary ring, presented at the *24th International Symposium on Space Flight Dynamics*, Laurel, Maryland, USA, 2014.
2. Siminski, J., Montenbruck, O., Fiedler, H., Schildknecht, T., Short-arc tracklet association for geostationary objects, *Advances in Space Research*, Vol. 53 (8), 2014.
3. Battin, R.H., *An introduction to the mathematics and methods of astrodynamics*, American Institute of Aeronautics and Astronautics, rev. ed. edition, 1999.
4. Gooding, R.H., A procedure for the solution of Lambert's orbital boundary-value problem, *Celestial Mechanics and Dynamical Astronomy*, Vol. 48 (2), 145-165, 1990.
5. Schumacher, P.W. Jr., Wilkins, M.P., Roscoe, C.W.T., Parallel algorithm for track initiation for optical space Surveillance, presented at the *6th European Conference on Space Debris*, Darmstadt, Germany, 2013.
6. Schneider, M.D., Bayesian linking of geosynchronous orbital debris tracks as seen by the Large Synoptic Survey Telescope, *Advances in Space Research*, Vol. 49 (4), 655-666, 2013.
7. Ansalone, L., Curti., F., A genetic algorithm for initial orbit determination from a too short arc optical observation, *Advances in Space Research*, Vol. 52 (3),477-489, 2013.
8. Roscoe, C.W.T., Schumacher Jr., P.W., Wilkins, M.P., Parallel track initiation for optical space surveillance using range and range-rate bounds, presented at the *AIAA/AAS Astrodynamics Specialist Conference*, Hilton Head, South Carolina, USA, 2013.
9. Schildknecht, T., Hugentobler, U., Ploner, M., Optical surveys of space debris in GEO, *Advances in Space Research*, Vol. 23 (1), 1999.
10. Flohrer, T., Optical Survey Strategies and their Application to Space Surveillance, *Geodätisch-Geophysikalische Arbeiten in der Schweiz*, Schweizerische Geodätische Kommission,Vol. 87, 2012.